Chemical Science

ROYAL SOCIETY OF CHEMISTRY

EDGE ARTICLE

View Article Online
View Journal | View Issue

Cite this: *Chem. Sci.*, 2022, **13**, 9940

All publication charges for this article have been paid for by the Royal Society of Chemistry

Received 25th February 2022
Accepted 28th July 2022

DOI: 10.1039/d2sc01175a

rsc.li/chemical-science

Electrochemically-promoted synthesis of benzo[*b*]thiophene-1,1-dioxides *via* strained quaternary spirocyclization†

Ruitao Li,[a] Dafu Yuan,[a] Mengqi Ping,[a] Yuyi Zhu,[b] Shaofei Ni,[b] Ming Li,[a] Lirong Wen [a] and Lin-Bao Zhang *[a]

We report an approach for the synthesis of benzothiophene motifs under electrochemical conditions by the reaction of sulfonhydrazides with internal alkynes. Upon the formation of a quaternary spirocyclization intermediate by the selective *ipso*-addition instead of an *ortho*-attack, the S-migration process was rationalized to lead to the products. Computational studies revealed the selectivity and the compatibility of drug molecules showcased the potential application of the protocols.

Introduction

Benzothiophenes have diverse applications in medicinal chemistry and materials science, furthermore, they arepresent in many natural products.[1] Consequently, the development of efficient methods for the construction of benzothiophene and its derivatives is of great importance.[2] Among these strategies, the intermolecular coupling of aromatic substrates with alkynes presents a straightforward route that benefits from step- and atom-economy.[3] However, the site selectivity of the above-mentioned protocol can be problematic for *meta*-substituted substrates with a mixture of products formed. In addition, the construction of benzothiophene motifs demands metal catalysts, elaborate starting materials, and harsh reaction conditions, reducing the efficiency of the existing protocols.[4] Thus, developing novel and green methods for such functional benzothiophene derivatives will be highly desirable.

The development of radical chemistry has drawn wide attention as it offers diverse and unique reaction pathways in synthetic chemistry.[5] Recently, intramolecular radical involved transformations toward the *ortho*- or *ipso*-carbon of the benzene ring have been extensively investigated, thus producing valuable molecular scaffolds by convenient synthetic means (Scheme 1a).[6] The *ipso*-counterpart provides unusual means for achieving the attainable products *via* a highly versatile spirocyclic intermediate compared to the *ortho*-addition strategy (**A** *vs.* **B**). In fact, the synthetic diversity of the spirocyclic pathway has successfully been demonstrated by the oxidative or reductive dearomative process,[7] as well as by various migratory reactions.[8] In this context, the Cho group developed spirocyclization reactions by applying iminyl radicals, respectively *via* a photocatalytic *ipso*-attack process (Scheme 1b).[9] Nevado and co-workers revealed the *ipso*-reactivity of sulfamidyl radicals with subsequent aryl migration.[10] The group of Chang showcased an approach of visible-light-induced selective C(sp^2)–H amidative cyclization to furnish δ-benzolactams *via* selective *ipso*-addition of amidyl radicals (Scheme 1c).[11]

On the other hand, organic electrochemistry has attracted broad interest as an enabling synthetic tool by the advantages of

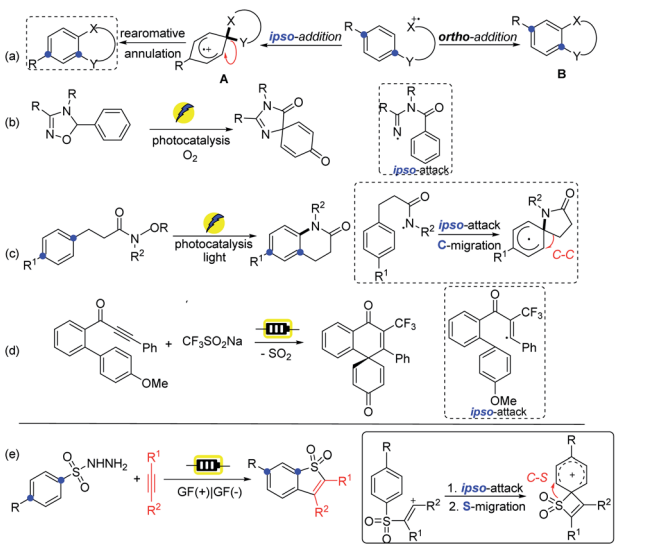

Scheme 1 The developed strategy involving an *ipso*-attack pathway (a–e).

[a]*State Key Laboratory Base of Eco-Chemical Engineering, College of Chemistry and Molecular Engineering, Qingdao University of Science & Technology, Qingdao, 266042, P. R. China. E-mail: zhang_linbao@126.com*

[b]*Department of Chemistry, Shantou University, Shantou, Guangdong, 515063 P. R. China*

† Electronic supplementary information (ESI) available. CCDC 2044891, 2044867 and 2171791. For ESI and crystallographic data in CIF or other electronic format see https://doi.org/10.1039/d2sc01175a

traceless electrons as a green reagent.[12] It can also promote dehydrogenative processes through H_2 release without the requirement of metal catalysts or chemical oxidants.[13] Moreover, the convenient tunability of the potential of the reaction system provides a fine handle to precisely harness redox transformations.[14] Recently, the group of Ackermann revealed an efficient approach for electrooxidative dearomatization of biaryls through radical spirocyclization *via* the *ipso*-attack route (Scheme 1d).[15] In our previous work, we have reported regio- and stereoselective electrochemical syntheses of sulfonylated enethers, which lead to benzo[*b*]thiophene-1,1-dioxides *via* the *ortho*-attack process.[16] Hence, our interest in electrochemical transformation and green chemistry prompts us to develop a new strategy for the direct formation of such benzothiophene motifs *via* an alkenyl radical intermediate followed by the selective *ipso*-addition instead of the *ortho*-attack pathway, which underwent S-migration *via* more strained quaternary spirocyclization (Scheme 1e).[17]

Results and discussion

Initial studies to determine the optimal reaction conditions were performed using 1-propynylbenzene (**1a**) to react with 4-methylbenzenesulfonhydrazide (**2a**) in HFIP under electrochemical anodic oxidation conditions (Table 1). Gratifyingly, the benzo[*b*]thiophene-1,1-dioxide (**3aa**) was obtained with a yield of 75%, using graphite felt (GF) electrodes under 5.0 mA constant current electrolysis in an undivided electrolytic cell at room temperature with Et_4NPF_6 as the electrolyte and HFIP/CH_3NO_2 as the co-solvent (Table 1, entry 1). Various reaction conditions were explored and it was found that both increasing and decreasing the constant current would lead to decreased reaction yields (Table 1, entries 2 and 3). The electrode material had an important impact on this reaction. Lower yields were obtained when the GF was replaced by a platinum cathode or a nickel foam cathode, giving **3aa** in 51% and 47% yields, respectively (Table 1, entries 4 and 5). As for the choice of electrolytes, the results revealed that other electrolytes such as $^nBu_4NPF_6$ or Me_4NPF_6 did not give superior yields (Table 1, entries 6 and 7). In addition, diminished reaction yields were achieved when HFIP was replaced with other solvents, such as DCM, DCE, THF and TFE (Table 1, entries 8–11), indicating that HFIP was crucial for the transformation, and this might be due to the fact that HFIP increased the reactivity of the carbocation intermediates involved in this process.[18] A control experiment showed that **3aa** was not generated without electricity (Table 1, entry 12). When the reaction was conducted under an air atmosphere (Table 1, entry 13), the yield was only 30%, indicating that the O_2 in air might quench the sulfonyl radical in the reaction process.

With the optimal reaction conditions confirmed, a series of alkynes were first used to systematically examine the general protocol. The results are presented in Scheme 2. The reaction showed a broad compatibility with various alkyl groups of the internal alkynes (**3aa–3qa**). In addition, the structure of **3aa** was further confirmed by X-ray crystallography analysis (see the ESI for details; CCDC: 2044891†). The unsymmetrical alkynes bearing a benzene ring and long chain alkyl groups resulted in **3aa–3ka** with yields of 75–39%. In addition, we speculate that the products were mixed with regioisomers and the ratio was determined through ^{1}H NMR analysis (**3ca′–3ka′**, see the ESI†

Table 1 Identification of reaction conditions[a]

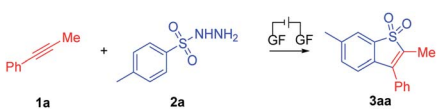

1a 2a 3aa

Entry	Deviation from standard conditions	Yield[b] (%)
1	None	75
2	3 mA, 13 h	70
3	10 mA, 4 h	65
4	Pt plate cathode	51
5	Nickel foam cathode	47
6	$^nBu_4NPF_6$ instead of Et_4NPF_6	64
7	Me_4NPF_6 instead of Et_4NPF_6	69
8	DCM instead of HFIP	62
9	DCE instead of HFIP	60
10	THF instead of HFIP	38
11	TFE instead of HFIP	Trace
12	No electric current	n.r
13	Under air	30

[a] Reaction conditions: **1a** (0.2 mmol), **2a** (0.6 mmol), Et_4NPF_6 (0.2 mmol), HFIP (4.7 mL), CH_3NO_2 (0.3 mL), graphite felt anode (10 mm × 10 mm × 5 mm), constant current = 5.0 mA, RT, 8 h, undivided cell (7.46 F, faradaic efficiency: 42%). [b] Isolated yield.

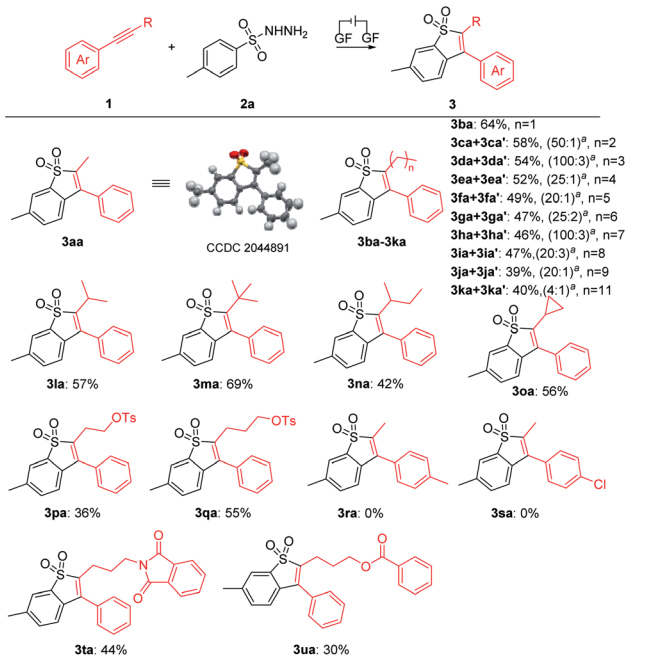

Scheme 2 Substrate scope of **1**. General reaction conditions: **1** (0.2 mmol), **2a** (0.6 mmol), Et_4NPF_6 (0.2 mmol), HFIP (4.7 mL), CH_3NO_2 (0.3 mL), graphite felt anode (10 mm × 10 mm × 5 mm), constant current = 5.0 mA, RT, 8 h, undivided cell. [a]The ratio was determined by ^{1}H NMR analysis.

for details). For substrates bearing isopropyl (**1la**), *tert*-butyl (**1ma**), *sec*-butyl (**1na**) and cyclopropyl (**1oa**), the corresponding products **3la–3oa** were smoothly delivered with yields of 69–42%, which indicated that the steric hindrance factor did not influence the efficiency of the electrochemical transformations. The alkane terminal OTs group was also compatible with the reaction system, providing corresponding products **3pa** and **3qa** in 36% and 55% yields, respectively. Disappointingly, we did not detect the products **3ra** and **3sa** when employing internal alkynes containing the methyl or chlorine group, possibly due to their relatively lower oxidation potential (see ESI, Fig. S3†). Protected amine (**3ta**) and ester (**3ua**) were smoothly delivered with yields of 44% and 30%, respectively. It should be noted that trace byproducts consistent with reduction of the benzothiophene core to the corresponding dihydrobenzothiophene were detected (see the ESI† for details).

Furthermore, the scope of aryl internal alkynes was further investigated, as summarized in Scheme 3. Similarly, the structure of **3Aa** was also confirmed by X-ray crystallography analysis (see the ESI† for details; CCDC: 2044867). We found that functional groups including methyl, ethyl and *tert*-butyl were well tolerated, generating the products **3Ba–3Da** in 43–64% yields. Moreover, halide substituents, including F, Cl and Br at the *para*-position of the benzene ring did not inhibit the reaction, affording **3Ea**, **3Fa** and **3Ga** in yields of 58%, 49% and 44%, respectively. The unsymmetric aryl alkyne (**1I**) underwent the electrochemical annulation to give **3Ia** and **3Ia′** with yields of 26% and 24%, respectively. In addition, the structure of **3la′** was further confirmed by X-ray crystallography analysis (see the ESI for details; CCDC: 2171791†). Unfortunately, the trial of the (hetero)cyclic alkynes under the conditions was unsuccessful.

Subsequently, the scope of arylsulfonyl hydrazides was explored as summarized in Scheme 4. We found that for benzenesulfonyl hydrazides bearing electron-donating groups such as ethyl (**2b**), the electron effect played a significant role in this transformation, as propyl (**2c**), cyclohexyl (**2d**) and *tert*-butyl (**2e**) at the *para*-position of the benzene ring underwent the transformation smoothly with yields of 51–69%. 3-Methylbenzenesulfonohydrazide **2f** reacted well with **1a**, producing corresponding rearrangement product **3af** in a yield of 56%. Moreover, the sulfonyl hydrazine **2g** decorated with 2-naphthalene finally provided naphtho[1,2-*b*]thiophene derivative **3ag** in moderate yield. We found that electron-donating groups such as methoxy (**2h**) could enable the reaction, while the electron-withdrawing substituent Cl (**2i**) at the same position of the benzene ring totally inhibited the electrolysis reaction.

To demonstrate the practicability of the reaction, a 5.0 mmol scale reaction of **1a** with **2a** was conducted, affording **3aa** in 82% yield under the conditions (Scheme 5a). Moreover, the triazo group was easily introduced under the reaction of **3qa** with sodium azide, which could be further functionalized *via* the click reaction (Scheme 5b).[19] It is particularly noteworthy that a series of natural products and pharmaceutical motifs such as indometacin, ibuprofen, gemfibrozil, loxoprofen,

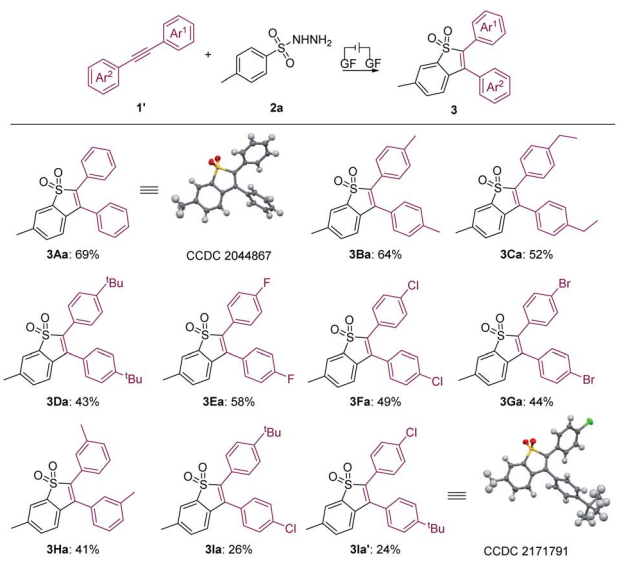

Scheme 3 Substrate scope of **1′**. General reaction conditions: **1′** (0.2 mmol), **2a** (0.6 mmol), Et_4NPF_6 (0.2 mmol), HFIP (4.7 mL), CH_3NO_2 (0.3 mL), graphite felt anode (10 mm × 10 mm × 5 mm), constant current = 5.0 mA, RT, 8 h, undivided cell.

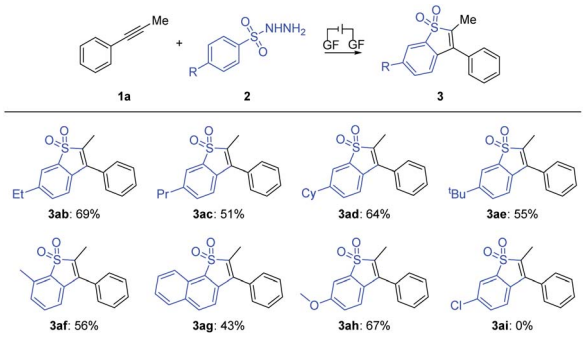

Scheme 4 Substrate scope of **2**. General reaction conditions: **1a** (0.2 mmol), **2** (0.6 mmol), Et_4NPF_6 (0.2 mmol), HFIP (4.7 mL), CH_3NO_2 (0.3 mL), graphite felt anode (10 mm × 10 mm × 5 mm), constant current = 5.0 mA, RT, 8 h, undivided cell.

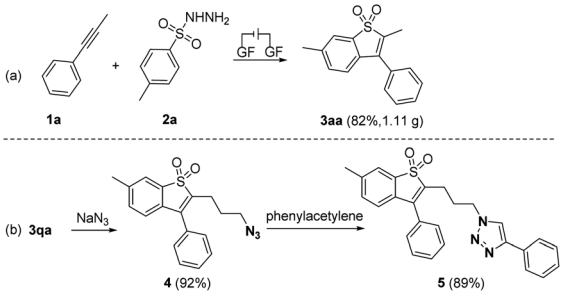

Scheme 5 (a) Gram-scale reaction. Reaction conditions: **1a** (5 mmol), **2a** (15 mmol), Et_4NPF_6 (5 mmol), HFIP (117.5 mL), CH_3NO_2 (7.5 mL), graphite felt anode (40 mm × 10 mm × 15 mm), constant current = 5.0 mA, RT, 67 h, undivided cell. (b) Functionalization of **3qa**. Reaction conditions: step 1, **3qa** (0.2 mmol), NaN_3 (0.24 mmol), DMF (1.1 mL), RT; step 2, **4** (0.2 mmol), phenylacetylene (0.26 mmol), $CuSO_4 \cdot 5H_2O$ (0.02 mmol), sodium ascorbate (0.05 mmol), THF (2.5 mL), H_2O (2.5 mL), RT, overnight.

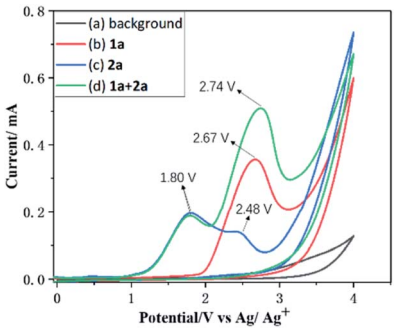

Fig. 1 Results of the cyclic voltammetry studies. Conditions: a glassy carbon working electrode, aqueous kit-Ag/Ag^+ reference electrode, and a platinum wire counter electrode, Et_4NPF_6 (0.01 M in CH_3CN), 100 mV s^{-1} scan rate with **1a** (0.02 M); **2a** (0.01 M); **1a** (0.02 M) + **2a** (0.01 M); background.

lambdacyhalothric acid, naproxen and isoxepac could undergo nucleophilic attack by **3qa**, generating benzo[*b*]thiophene-1,1-dioxide linked drug derivatives 6–12 in good yields (see ESI, Scheme S2†).

To gain some insights into the reaction mechanism, control experiments were performed. First of all, cyclic voltammetry (CV) experiments were performed on **1a** and **2a** and the results revealed that the oxidation peak of **1a** emerged at 2.67 V, which is consistent with the observation of the radical cation.[20] However the oxidation peaks of **2a** emerged at 1.80 V and 2.48 V, respectively, indicating that **2a** was oxidized preferentially at the anode (Fig. 1).

Control experiments were performed to probe the mechanism (Scheme 6), and the addition of radical scavengers, butylated hydroxytoluene (BHT, 3.0 equiv. Scheme 6a) and 2,2,6,6-tetramethylpiperidinooxy (TEMPO, 3.0 equiv. Scheme 6b) totally inhibited the reaction, indicating that the radical pathway was involved in the process. In addition, compound **13** was isolated in 55% yield and **14** was detected by HPLC-MS analysis (see ESI, Fig. S4†). Moreover, complex **15** was isolated in 79% yield, when 1,1-diphenylethylene (3.0 equiv. Scheme 6c) was subjected to the reaction, further demonstrating the

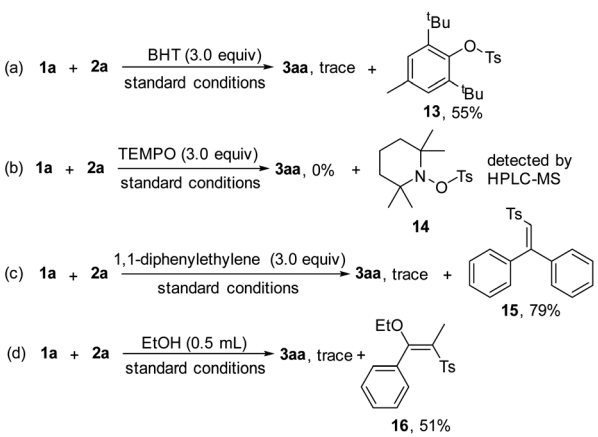

Scheme 6 Control experiments (a–d).

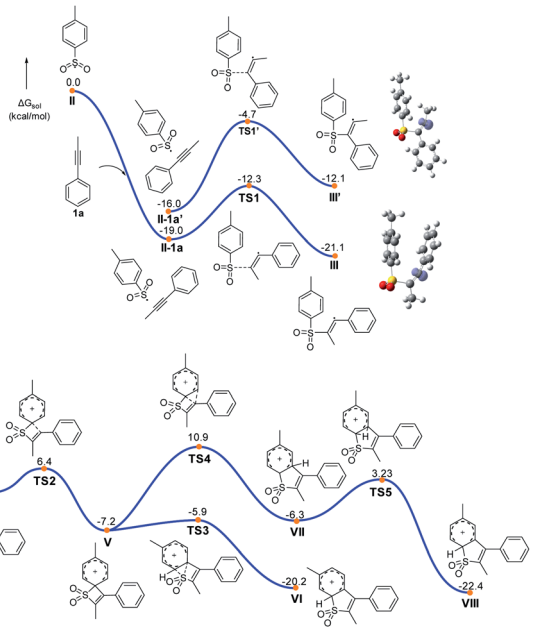

Fig. 2 DFT calculations.

existence of the sulfonyl radical. We found that sulfonylated enether **16** was produced in 51% yield by adding EtOH as the co-solvent under the electrochemical conditions (Scheme 6d), which might act as indirect evidence of the alkenyl cation in the process.[16]

On the basis of our experiments, a plausible route is presented and the theoretically calculated results are presented in Fig. 2 and Scheme 7. The sulfonyl radical **II** formation involved deprotonation, anodic oxidation and nitrogen liberation. Then the sulfonyl radical **II** reacted with **1a** to form the alkenyl radical **III**, which underwent further anodic oxidation to produce the alkenyl cation intermediate **IV** and HFIP in the solvent can play the role of stabilizing positive ions. As shown in Fig. 2, the free

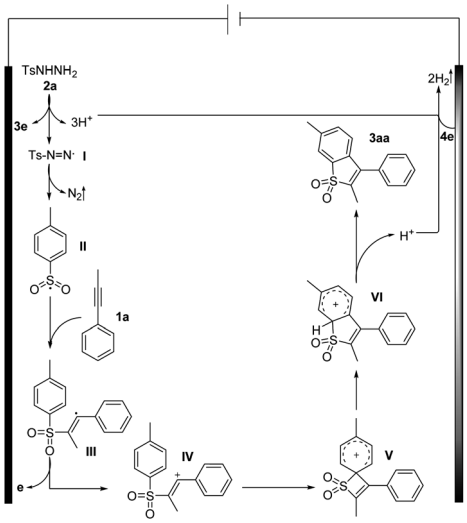

Scheme 7 Proposed mechanism.

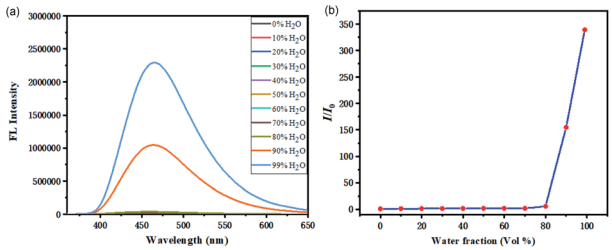

Fig. 3 Fluorescence intensities and dependence of I/I_0 ratios of **3Aa** (a and b) in DMSO/water mixed solvent with different water fractions. Concentration: 10^{-5} M.

energy barrier for this radical addition process *via* **TS1** is calculated to be 6.7 kcal mol^{-1}, about 8 kcal mol^{-1} lower than that of the regioselective transition state **TS1′**, agreeing well with the experimentally observed regioselectivity. Intermediate **IV** undergoes intra-molecular cyclization *via* transition state **TS2** (Fig. 2) to form quaternary spirocyclization species **V**, which then rapidly undergoes ring expansion involving 1,2-S-migration to give **VI**. The calculated reaction barriers for the cyclization and 1,2-S-migration processes are 6.4 and 1.3 kcal mol^{-1}, respectively, which are affordable under the current reaction conditions. Further oxidation and deprotonation processes gave the target product **3aa**. The ring expansion transition state **TS4** involving 1,2-C-migration is also located with the reaction barrier calculated to be 18.1 kcal mol^{-1}, which is rather higher than that of S-migration.

The fluorescent properties of **3Aa** were further studied in a solvent mixture of DMSO and water (Fig. 3a). These fluorophores showed relatively weak blue fluorescence in DMSO, and the emission peaks are slightly red-shifted with the increase of water fraction. Initially, addition of water had little effect on the emission intensity. When the water fraction was greater than 80%, the fluorescence intensity increased dramatically (Fig. 3b), which indicated that **3Aa** exhibits good aggregation-induced emission.[21]

The fluorescent emission of these compounds (**3Aa–3Ia′**) is obviously blue-shifted or red-shifted in solution (Fig. 4a). They exhibit strong blue emission with maximum emission wavelength around 334–442 nm. Further investigation reveals that these benzothiophene derivatives are good emitters with CIE coordinates as follows: **3Aa** (0.16, 0.13), **3Ba** (0.18, 0.10), **3Ca** (0.18, 0.12), **3Da** (0.14, 0.10), **3Ea** (0.15, 0.07), **3Fa** (0.17, 0.10), **3Ga** (0.16, 0.14), **3Ha** (0.15, 0.08), **3Ia** (0.16, 0.16), and **3Ia′** (0.16, 0.13) (Fig. 4b).

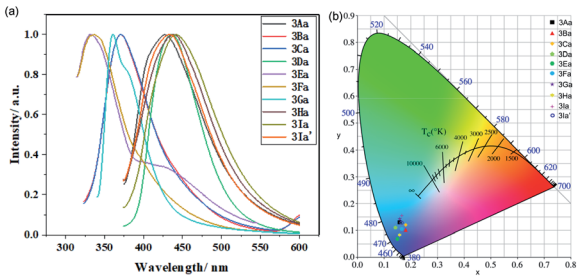

Fig. 4 (a) Normalized liquid-state fluorescence spectra of **3Aa–3Ia′**. (b) The CIE coordinates of **3Aa–3Ia′**.

Inspired by the potential biological applications of benzothiophene,[22] we performed fluorescence imaging of HeLa cells incubated with **3Ha** for 10 min, with excitation at 405 nm and the collection wavelength range was 420–460 nm. The result showed that green fluorescence was observed throughout the whole cytoplasm (see ESI, Fig. S5†).[23]

Conclusions

In summary, we have developed an efficient electrochemical method for the synthesis of benzothiophene dioxides by the reaction of sulfonhydrazides with internal alkynes at room temperature in undivided cells by constant current electrolysis.[24] We observed that selective *ipso*-addition instead of the *ortho*-attack pathway led to strained quaternary spirocyclization, which produced the products *via* the S-migration process. The protocol avoided the requirement of transition metal catalysts or stoichiometric amounts of oxidants, and a variety of functional groups were tolerated. Moreover, gram-scale experiments and the transformation involving drug molecules might provide an effective route for the synthesis of value-added compounds.

Data availability

All experimental data and detailed experimental procedures are available in the ESI.†

Author contributions

R. L. and D. Y. conceived and performed the majority of experiments. M. P. performed a part of the research work. S. N. and Y. Z. performed DFT calculations. M. L. and L.-R. W. polished the manuscript. L.-B. Z. conceived and directed the project and wrote the paper. All the authors discussed the results and commented on the manuscript.

Conflicts of interest

There are no conflicts to declare.

Acknowledgements

We thank the Natural Science Foundation of China (21801152 and 21572110) and the Natural Science Foundation of Shandong Province (ZR2019BB005 and ZR2019MB010) for financial support. We thank the Youth Innovation Science and Technology Plan of Colleges and Universities in Shandong Province (2021KJ076). L. B. Zhang acknowledges the Hong Kong Scholars Program (XJ2020013).

Notes and references

1 (*a*) R. S. Keri, K. Chand, S. Budagumpi, S. B. Somappa, S. A. Patil and B. M. Nagaraja, *Eur. J. Med. Chem.*, 2017, **138**, 1002–1033; (*b*) A. J. Seed, K. J. Toyne, J. W. Goodby and M. Hird, *J. Mater. Chem.*, 2000, **10**, 2069; (*c*) I. Fouad, Z. Mecbal, K. I. Chane-Ching, A. Adenier, F. Maurel, J.-J. Aaron, P. Vodicka, K. Cernovska, V. Kozmik and J. Svoboda, *J. Mater. Chem.*, 2004, **14**, 1711–1721; (*d*) J. W. Ellingboe, T. R. Alessi, T. M. Dolak, T. T. Nguyen, J. D. Tomar, F. Guzzo, J. F. Bagli and M. L. Mccaleb, *J. Med. Chem.*, 1992, **35**, 1176–1183; (*e*) M. S. Malamas, J. Sredy, C. Moxham, A. Katz, W. Xu, R. Mcdevitt, F. O. Adebayo, D. R. Sawicki, L. Seestaller, D. Sullivan and J. R. Taylor, *J. Med. Chem.*, 2000, **43**, 1293–1310.

2 (*a*) Y. Ma, K. Wang, D. Zhang and P. Sun, *Adv. Synth. Catal.*, 2019, **361**, 597–602; (*b*) I. Nakamura, T. Sato and Y. Yamamoto, *Angew. Chem., Int. Ed.*, 2006, **45**, 4473–4475; (*c*) E. Ramesh, T. Guntreddi and A. K. Sahoo, *Eur. J. Org. Chem.*, 2017, **2017**, 4405–4413; (*d*) R. Che, Z. Wu, Z. Li, H. Xiang and X. Zhou, *Chem.–Eur. J.*, 2014, **20**, 7258–7261; (*e*) H. Ebata, E. Miyazaki, T. Yamamoto and K. Takimiya, *Org. Lett.*, 2007, **9**, 4499–4502; (*f*) B. L. Flynn, P. Verdier-Pinard and E. Hamel, *Org. Lett.*, 2001, **3**, 651–654.

3 (*a*) E. Ramesh, M. Shankar, S. Dana and A. K. Sahoo, *Org. Chem. Front.*, 2016, **3**, 1126–1130; (*b*) R. Zhu, J. Wei and Z. Shi, *Chem. Sci.*, 2013, **4**, 3706–3711; (*c*) R. C. Larock, E. K. Yum, M. J. Doty and K. K. C. Sham, *J. Org. Chem.*, 1995, **60**, 3270–3271.

4 S. Ejaz, M. Zubair, K. Rizwan, I. Karakaya, T. Rasheed and N. Rasool, *Curr. Org. Chem.*, 2021, **25**, 40–67.

5 (*a*) T. Pintauer and K. Matyjaszewski, *Chem. Soc. Rev.*, 2008, **37**, 1087–1097; (*b*) A. Studer and D. P. Curran, *Angew. Chem., Int. Ed.*, 2016, **55**, 58–102; (*c*) K. J. Romero, M. S. Galliher, D. A. Pratt and C. R. J. Stephenson, *Chem. Soc. Rev.*, 2018, **47**, 7851–7866; (*d*) H. Wang, W. Shi, Y. Li, M. Yu, Y. Gao and A. Lei, *CCS Chem.*, 2020, **2**, 1710–1717.

6 (*a*) C. L. Perrin, *J. Org. Chem.*, 2021, **86**, 14245–14249; (*b*) C. L. Perrin and G. A. Skinner, *J. Am. Chem. Soc.*, 1971, **93**, 3389–3394; (*c*) C. L. Perrin, *J. Org. Chem.*, 1971, **36**, 420–425; (*d*) X. Liu, F. Xiong, X. Huang, L. Xu, P. Li and X. Wu, *Angew. Chem., Int. Ed.*, 2013, **52**, 6962–6966; (*e*) Z.-M. Chen, W. Bai, S.-H. Wang, B.-M. Yang, Y.-Q. Tu and F.-M. Zhang, *Angew. Chem., Int. Ed.*, 2013, **52**, 9781–9785; (*f*) A. Bunescu, Q. Wang and J. Zhu, *Angew. Chem., Int. Ed.*, 2015, **54**, 3132–3135.

7 (*a*) J. Boivin, M. Yousfi and S. Z. Zard, *Tetrahedron Lett.*, 1997, **38**, 5985–5988; (*b*) H. Ohno, S.-i. Maeda, M. Okumura, R. Wakayama and T. Tanaka, *Chem. Commun.*, 2002, 316–317; (*c*) H. Ohno, M. Okumura, S.-i. Maeda, H. Iwasaki, R. Wakayama and T. Tanaka, *J. Org. Chem.*, 2003, **68**, 7722–7732; (*d*) H. Iwasaki, T. Eguchi, N. Tsutsui, H. Ohno and T. Tanaka, *J. Org. Chem.*, 2008, **73**, 7145–7152; (*e*) T. Yamada, Y. Ozaki, M. Yamawaki, Y. Sugiura, K. Nishino, T. Morita and Y. Yoshimi, *Tetrahedron Lett.*, 2017, **58**, 835–838; (*f*) A. R. Flynn, K. A. McDaniel, M. E. Hughes, D. B. Vogt and N. T. Jui, *J. Am. Chem. Soc.*, 2020, **142**, 9163–9168; (*g*) H. Takeuchi, S. Inuki, K. Nakagawa, T. Kawabe, A. Ichimura, S. Oishi and H. Ohno, *Angew. Chem., Int. Ed.*, 2020, **59**, 21210–21215; (*h*) L. Wu, Y. Hao, Y. Liu, H. Song and Q. Wang, *Chem. Commun.*, 2020, **56**, 8436–8439.

8 (*a*) N. Fuentes, W. Kong, L. Fernández-Sánchez, E. Merino and C. Nevado, *J. Am. Chem. Soc.*, 2015, **137**, 964–973; (*b*) W. Kong, M. Casimiro, E. Merino and C. Nevado, *J. Am. Chem. Soc.*, 2013, **135**, 14480–14483; (*c*) H. Jiang and A. Studer, *Angew. Chem., Int. Ed.*, 2018, **57**, 10707–10711; (*d*) N. Radhoff and A. Studer, *Angew. Chem., Int. Ed.*, 2021, **60**, 3561–3565; (*e*) Z. Wu, D. Wang, Y. Liu, L. Huan and C. Zhu, *J. Am. Chem. Soc.*, 2017, **139**, 1388–1391; (*f*) X. Wu, M. Wang, L. Huan, D. Wang, J. Wang and C. Zhu, *Angew. Chem., Int. Ed.*, 2018, **57**, 1640–1644; (*g*) X. Wu and C. Zhu, *Acc. Chem. Res.*, 2020, **53**, 1620–1636; (*h*) Z.-M. Chen, X.-M. Zhang and Y.-Q. Tu, *Chem. Soc. Rev.*, 2015, **44**, 5220–5245; (*i*) M. Huynh, M. D. Abreu, P. Belmont and E. Brachet, *Chem.–Eur. J.*, 2021, **27**, 3581–3607; (*j*) Y.-R. Chen and W.-L. Duan, *J. Am. Chem. Soc.*, 2013, **135**, 16754–16757.

9 V. K. Soni, H. S. Hwang, Y. K. Moon, S. W. Park, Y. You and E. J. Cho, *J. Am. Chem. Soc.*, 2019, **141**, 10538–10545.

10 W. Kong, E. Merino and C. Nevado, *Angew. Chem., Int. Ed.*, 2014, **53**, 5078–5082.

11 H. Keum, H. Jung, J. Jeong, D. Kim and S. Chang, *Angew. Chem., Int. Ed.*, 2021, **60**, 25235–25240.

12 (*a*) C. Ma, P. Fang and T.-S. Mei, *ACS Catal.*, 2018, **8**, 7179–7189; (*b*) C. Ma, P. Fang, D. Liu, K.-J. Jiao, P.-S. Gao, H. Qiu and T.-S. Mei, *Chem. Sci.*, 2021, **12**, 12866–12873; (*c*) K.-J. Jiao, Y.-K. Xing, Q.-L. Yang, H. Qiu and T.-S. Mei, *Acc. Chem. Res.*, 2020, **53**, 300–310; (*d*) H. Wang, X. Gao, Z. Lv, T. Abdelilah and A. Lei, *Chem. Rev.*, 2019, **119**, 6769–6787; (*e*) Y. Yuan, J. Yang and A. Lei, *Chem. Soc. Rev.*, 2021, **50**, 10058–10086; (*f*) T. H. Meyer, I. Choi, C. Tian and L. Ackermann, *Chem*, 2020, **6**, 2484–2496; (*g*) R. C. Samanta, T. H. Meyer, I. Siewert and L. Ackermann, *Chem. Sci.*, 2020, **11**, 8657–8670.

13 (*a*) C. Zhu, N. W. J. Ang, T. H. Meyer, Y. Qiu and L. Ackermann, *ACS Cent. Sci.*, 2021, **7**, 415–431; (*b*) S.-H. Shi, Y. Liang and N. Jiao, *Chem. Rev.*, 2021, **121**, 485–505; (*c*) L. Ackermann, *Acc. Chem. Res.*, 2020, **53**, 84–104; (*d*) S. D. Minteer and P. Baran, *Acc. Chem. Res.*, 2020, **53**, 545–546; (*e*) P. Xiong and H.-C. Xu, *Acc. Chem. Res.*, 2019, **52**, 3339–3350; (*f*) W. Zhang and S. Lin, *J. Am. Chem. Soc.*, 2020, **142**, 20661–20670; (*g*) J. C. Siu, N. Fu and S. Lin, *Acc. Chem. Res.*, 2020, **53**, 547–560; (*h*) Y. Kawamata and P. S. Baran, *Joule*, 2020, **4**, 701–704.

14 (*a*) C. Kingston, M. D. Palkowitz, Y. Takahira, J. C. Vantourout, B. K. Peters, Y. Kawamata and P. S. Baran, *Acc. Chem. Res.*, 2020, **53**, 72–83; (*b*) M. Yan, Y. Kawamata and P. S. Baran, *Chem. Rev.*, 2017, **117**, 13230–13319; (*c*) C. Huang, Z.-Y. Li, J. Song and H.-C. Xu, *Angew. Chem., Int. Ed.*, 2021, **60**, 11237–11241; (*d*) L. F. T. Novaes, J. Liu, Y. Shen, L. Lu, J. M. Meinhardt and S. Lin, *Chem. Soc. Rev.*, 2021, **50**, 7941–8002; (*e*) N. Fu, G. S. Sauer, A. Saha, A. Loo and S. Lin, *Science*, 2017, **357**,

575–579; (*f*) Z. Zhang, L. Zhang, X. Zhang, J. Yang, Y. Yin, Y. Jiang, C. Zeng, G. Lu, Y. Yang and F. Mo, *Chem. Sci.*, 2020, **11**, 12021–12028; (*g*) Y. Liang, S.-H. Shi, R. Jin, X. Qiu, J. Wei, H. Tan, X. Jiang, X. Shi, S. Song and N. Jiao, *Nat. Catal.*, 2021, **4**, 116–123; (*h*) Y. Yuan, Y. Cao, Y. Lin, Y. Li, Z. Huang and A. Lei, *ACS Catal.*, 2018, **8**, 10871–10875.

15 Y. Zhang, C. Ma, J. Struwe, J. Feng, G. Zhu and L. Ackermann, *Chem. Sci.*, 2021, **12**, 10092–10096.

16 W.-B. Du, N.-N. Wang, C. Pan, S.-F. Ni, L.-R. Wen, M. Li and L.-B. Zhang, *Green Chem.*, 2021, **23**, 2420–2426.

17 (*a*) Z. Kong, C. Pan, M. Li, L. Wen and W. Guo, *Green Chem.*, 2021, **23**, 2773–2777; (*b*) L.-B. Zhang, R.-S. Geng, Z.-C. Wang, G.-Y. Ren, L.-R. Wen and M. Li, *Green Chem.*, 2020, **22**, 16–21; (*c*) Z.-C. Wang, R.-T. Li, Q. Ma, J.-Y. Chen, S.-F. Ni, M. Li, L.-R. Wen and L.-B. Zhang, *Green Chem.*, 2021, **23**, 9515–9522; (*d*) L.-R. Wen, N.-N. Wang, W.-B. Du, M.-Z. Zhu, C. Pan, L.-B. Zhang and M. Li, *Chin. J. Chem.*, 2021, **39**, 1831–1837; (*e*) L.-R. Wen, Y. Rao, M. Zhu, R. Li, J. Zhan, L. Zhang, L. Wang, M. Li, S. Pang and Z. Zhou, *Angew. Chem., Int. Ed.*, 2021, **60**, 17356–17361; (*f*) D.-F. Yuan, Z.-C. Wang, R.-S. Geng, G.-Y. Ren, J. S. Wright, S.-F. Ni, M. Li, L.-R. Wen and L.-B. Zhang, *Chem. Sci.*, 2022, **13**, 478–485; (*g*) L.-B. Zhang, Z.-C. Wang, S.-Z. Sun, S.-F. Ni, L.-R. Wen and M. Li, *Chin. J. Chem.*, 2018, **36**, 587–593.

18 (*a*) A. Berkessel, J. A. Adrio, D. Hüttenhain and J. M. Neudörfl, *J. Am. Chem. Soc.*, 2006, **128**, 8421–8426; (*b*) J. M. Ramos-Villaseñor, E. Rodríguez-Cárdenas, C. E. B. Díaz and B. A. Frontana-Uribe, *J. Electrochem. Soc.*, 2020, **167**, 155509.

19 P. Thirumurugan, D. Matosiuk and K. Jozwiak, *Chem. Rev.*, 2013, **113**, 4905–4979.

20 Z. Yang, F. Lu, H. Li, Y. Zhang, W. Lin, P. Guo, J. Wan, R. Shi, T. Wang and A. Lei, *Org. Chem. Front.*, 2020, **7**, 4064–4068.

21 Y. Fang, Y. Meng, C. Yuan, C. Du, K.-P. Wang, S. Chen and Z.-Q. Hu, *Spectrochimica Acta, Part A: Molecular and Biomolecular Spectroscopy*, 2022, **267**, 120575.

22 Y.-C. Jeong, S. I. Yang, E. Kim and K.-H. Ahn, *Tetrahedron*, 2006, **62**, 5855–5861.

23 (*a*) X. Cui, W. Cheng and X. Han, *J. Mater. Chem. B*, 2018, **6**, 8078–8084; (*b*) Q. Zhang, C. Fu, X. Guo, J. Gao, P. Zhang and C. Ding, *ACS Sens.*, 2021, **6**, 1138–1146.

24 During the submission stage of this paper, a similar electrochemical migratory cyclization was reported. Z. Shi, Y. Li, N. Li, W.-Z. Wang, H.-K. Lu, H. Yan, Y. Yuan, J. Zhu and K. Ye, *Angew. Chem., Int. Ed.*, 2022, **61**, DOI: **10.1002/anie.202206058**.